

Binary Systems as Resonance Detectors for Gravitational Waves

Lam Hui,^{1,2,3,*} Sean T. McWilliams,^{1,4,†} and I-Sheng Yang^{1,5,‡}

¹*Institute for Strings, Cosmology and Astroparticle Physics (ISCAP), Columbia University, New York, NY 10027*

²*Department of Physics, Columbia University, New York, NY 10027*

³*Columbia Astrophysics Laboratory, Columbia University, New York, NY 10027*

⁴*Department of Physics, Princeton University, Princeton, NJ 08544*

⁵*IOP and GRAPPA, Universiteit van Amsterdam,
Science Park 904, 1090 GL Amsterdam, Netherlands*

(Dated: June 4, 2018)

Gravitational waves at suitable frequencies can resonantly interact with a binary system, inducing changes to its orbit. A stochastic gravitational-wave background causes the orbital elements of the binary to execute a classic random walk, with the variance of orbital elements growing with time. The lack of such a random walk in binaries that have been monitored with high precision over long time-scales can thus be used to place an upper bound on the gravitational-wave background. Using periastron time data from the Hulse-Taylor binary pulsar spanning ~ 30 years, we obtain a bound of $h_c < 7.9 \times 10^{-14}$ at $\sim 10^{-4}$ Hz, where h_c is the strain amplitude per logarithmic frequency interval. Our constraint complements those from pulsar timing arrays, which probe much lower frequencies, and ground-based gravitational-wave observations, which probe much higher frequencies. Interesting sources in our frequency band, which overlaps the lower sensitive frequencies of proposed space-based observatories, include white-dwarf/supermassive black-hole binaries in the early/late stages of inspiral, and TeV scale preheating or phase transitions. The bound improves as (time span)⁻² and (sampling rate)^{-1/2}. The Hulse-Taylor constraint can be improved to $\sim 3.8 \times 10^{-15}$ with a suitable observational campaign over the next decade. Our approach can also be applied to other binaries, including (with suitable care) the Earth-Moon system, to obtain constraints at different frequencies. The observation of additional binary pulsars with the SKA could reach a sensitivity of $h_c \sim 3 \times 10^{-17}$.

PACS numbers: 04.30.-w 04.30.Db, 95.30.Sf

I. INTRODUCTION

The first direct detection of gravitational waves (GWs) will be a landmark event. With the advent of the Advanced Laser Interferometer Gravitational Wave Observatory (LIGO) and Advanced Virgo network of detectors in ~ 2015 , and the rapid progress of pulsar timing arrays (PTAs), it is likely that the next few years will see this breakthrough come to pass.

In this paper, we will investigate an alternative approach to GW detection, based on precision orbital monitoring of binary systems. The most promising binary systems are those with (at least) one pulsar member, although the way our method works and the frequencies that are probed differ significantly from the PTA method. PTAs probe gravitational waves that pass between the pulsars and us, distorting the arrival times of what would otherwise be very regular pulses. We are interested instead in how background GWs interact with the orbital dynamics of a binary system. We emphasize that we are not so much interested in the emission of GWs by the binary – an important subject in its own right – as in the changes to its orbital parameters due to

scattering with some external GW background.

The scattering is especially effective at GW frequencies that match a harmonic of the binary's orbital frequency, thereby inducing a resonance. For a circular orbit, resonance occurs at twice the orbital frequency. For eccentric orbits, resonance takes place to varying degrees at all harmonics of the orbital frequency, starting from the fundamental. Note that this scattering process is quite special and not frequently discussed. A binary is inevitably losing energy over time by emitting gravitational waves; the external GWs merely introduces a small modulation of this overall energy loss (for external GWs of a sufficiently small amplitude). Depending on the relative phase between the external gravitational wave and the binary, a constructive resonance slows down the energy loss, while a destructive resonance speeds it up. Immersed in a stochastic background of GWs, the binary orbital elements will thus execute a classic random walk on top of the secular decay due to its own GW emission. On average, the expected excursion of orbital elements due to GW scattering vanishes. However, the variance of the excursion is non-zero and in fact grows over time, as in Brownian motion. Such orbital excursions can therefore be used to detect GWs, and the lack of such excursions can be used to place bounds. We again emphasize the fundamental difference between our approach and that of PTAs, since we are interested in measuring actual changes in the binary's orbital parameters, rather than merely apparent changes due to the

*Electronic address: lhui@astro.columbia.edu

†Electronic address: stmcwill@princeton.edu

‡Electronic address: isheng.yang@gmail.com

presence of GWs along our line of sight.

Versions of this idea have been discussed in pioneering work by [1–6]. The subject lay dormant for many years, perhaps due in part to the focus shifting to PTAs in discussions of pulsars as a detection tool. We wish to revive the discussion by: (1) taking advantage of over 30 years of precision monitoring of the famed Hulse-Taylor binary, recognizing that the rms orbital excursion due to GW scattering increases with time, (2) generalizing earlier work by computing the random walk of a binary orbit with arbitrary eccentricity, due to scattering by any stochastic GW background, and (3) finding the minimum variance estimator for the stochastic GW power spectrum, given periastron time data; a main result is that the rms fluctuation in periastron time grows as (time span)^{3/2}. The approach we propose can be thought of as an astronomical version of Weber’s resonance bar [7].

The only data we thoroughly analyze in this paper is from the Hulse-Taylor (HT) system PSR B1913+16. It provides a current constraint on the stochastic GW background that is weaker than the one from the Doppler tracking of Cassini, and neither constraint is very restrictive. However, future observations of similar binary systems are expected to improve the constraint considerably. Our method can also be applied to other binary systems which have also been monitored with high precision over long time scales, such as the Earth-Moon and Earth-Sun systems. In Sec. V we discuss the prospects and challenges of obtaining constraints from them. We will use the term “detector binary” as the generic descriptor for the systems of interest.

II. FORMALISM

We limit our focus to a GW background that is stochastic in nature, i.e. during the course of observation, the GW signal is not dominated by a single source with a definite phase, but rather arises from a multitude of sources, contributing to a signal that is statistically stationary. For practical purposes, this means a Gaussian random field, although our calculation does not rely on Gaussianity. Because of our interest in PSR B1913+16, we are particularly interested in harmonics of its orbital frequency $f_{\text{HT}} \equiv 3.6 \times 10^{-5}$ Hz.

This frequency corresponds to the Hubble scale at a temperature of about 100 GeV. Early universe processes, such as preheating after low scale inflation or bubble collisions at the electroweak phase transition, generate a stochastic GW background at these frequencies [8–11]. However, more promising sources of GWs at these frequencies may come from the later universe, in particular from a large population of double white dwarf binaries in the early stages of inspiral, and from supermassive black-hole binaries in the late stages. These sources emit GWs at frequencies $f_r = 1.3 \times 10^{-4}$ Hz $[10^5 GMc^{-2}/a]^{3/2} [M_\odot/M]$, where f_r is the frequency in the source’s rest frame, a is the mean

orbital separation, and M is the total mass of the binary. Estimates by [12–16] suggest that the rms strain amplitude per logarithmic frequency from white dwarf binaries is roughly $h_c \sim 10^{-20} - 10^{-19} (f/f_{\text{HT}})^{-2/3}$, where f is the orbital frequency of interest, and the number of sources within the frequency width of interest (see below) is sufficiently large to give a GW background that is Gaussian random to good approximation.¹

Supermassive black-hole binaries constitute another promising source of GWs. However, the GWs generated by these systems at frequencies $\sim 10^{-4}$ Hz would not be stochastic in character, since the number of black-hole binaries potentially resonating with HT is much smaller. The interaction of the detector binary with GWs from these sources is therefore better characterized by individual events. In the course of each event, the relative phase between the source and the detector binary remains coherent; the detector orbital elements would therefore change in a secular rather than a stochastic fashion. Over time, the detector binary would encounter different, uncorrelated events, and thus there would still be a net random walk of sorts, if viewed over sufficiently long timescales. However, obtaining quantitative constraints on GWs of such a character would require a different calculation from the one presented here – a subject we hope to address in the future. In this paper, we focus instead on the classic random walk effect, relevant for GWs from double white-dwarf binaries or the early universe.

Let (X, Y, Z) define the frame of the detector binary, with the binary orbit lying in the X - Y plane. Let (x, y, z) define the frame of a particular gravitational wave train, with \hat{z} being the incident direction. We can go from (X, Y, Z) to (x, y, z) by performing three consecutive $Z - Y - Z$ Euler rotations. The last Euler rotation can be ignored since it is equivalent to rotating among the polarizations of the GWs, which we average over in any case. Thus, without loss of generality:

$$x = (X \cos \phi + Y \sin \phi) \cos \theta, \quad (1a)$$

$$y = Y \cos \phi - X \sin \phi, \quad (1b)$$

$$z = (X \cos \phi + Y \sin \phi) \sin \theta, \quad (1c)$$

where ϕ and θ are two Euler angles.

The induced relative acceleration $\vec{A} \equiv A_x \hat{x} + A_y \hat{y} + A_z \hat{z}$ of a binary system due to a gravitational wave incident

¹ Gaussian randomness can be checked, for instance, by comparing the connected 4th moment against the second moment squared. Demanding the former is small compared to the latter is equivalent to requiring no. of sources $\times \langle A^2 \rangle^2 / \langle A^4 \rangle \gg 1$, where A is the amplitude of the gravitational wave from a given source. For our application, the number of sources $\sim 10^{11}$ while $\langle A^2 \rangle^2 / \langle A^4 \rangle \sim 10^{-5}$.

from the \hat{z} direction is given by [6]

$$A_x = -R_{x0x0}x - R_{x0y0}y = \frac{1}{2} \left(\ddot{h}_{+x} + \ddot{h}_{\times y} \right), \quad (2a)$$

$$A_y = -R_{y0x0}x - R_{y0y0}y = \frac{1}{2} \left(\ddot{h}_{\times x} - \ddot{h}_{+y} \right), \quad (2b)$$

$$A_z = 0, \quad (2c)$$

where $R_{\mu\nu\alpha\beta}$ is the Riemann tensor, and h as the amplitude of the gravitational wave strain, with $+$ and \times subscripts denoting the two polarization states. Eq. (2) allows us to write down the time dependence of the energy,

$$\begin{aligned} \frac{dE}{dt} &= \mu (A_x \dot{x} + A_y \dot{y} + A_z \dot{z}) \\ &= \frac{\mu}{2} \left(\ddot{h}_{+}(x\dot{x} - y\dot{y}) + \ddot{h}_{\times}(x\dot{y} + y\dot{x}) \right), \end{aligned} \quad (3)$$

where $\mu \equiv \frac{m_1 m_2}{m_1 + m_2}$ is the reduced mass of the binary. Note that this gives the energy change solely induced by the incoming gravitational wave, which is on top of its original energy loss due to emission. Analogous expressions can be written down for the angular and center-of-mass linear momenta (see Appendix).

In Eq. (3), we can see that the quantities related to the binary motion are the quadrupole components. It is straightforward to obtain their Fourier expansions as

$$X(t)^2 = X_o^2 + \sum_{n=1}^{\infty} Q_{XX}(n) \cos(2\pi n f t), \quad (4a)$$

$$Y(t)^2 = Y_o^2 + \sum_{n=1}^{\infty} Q_{YY}(n) \cos(2\pi n f t), \quad (4b)$$

$$X(t)Y(t) = X_o Y_o + \sum_{n=1}^{\infty} Q_{XY}(n) \sin(2\pi n f t), \quad (4c)$$

where X_o and Y_o are constants, and f is the orbital frequency. The Q 's are the quadrupole moments [17]:

$$\begin{aligned} Q_{XX}(n) &= \frac{a^2}{n} \left(J_{n-2}(ne) - 2eJ_{n-1}(ne) \right. \\ &\quad \left. + 2eJ_{n+1}(ne) - J_{n+2}(ne) \right), \end{aligned} \quad (5a)$$

$$Q_{YY}(n) = -Q_{XX}(n) + \frac{4a^2}{n^2} J_n(ne), \quad (5b)$$

$$Q_{XY}(n) = \frac{a^2}{n} \sqrt{1-e^2} \left(J_{n-2}(ne) - 2J_n(ne) + J_{n+2}(ne) \right), \quad (5c)$$

where we use:

where a is the semi-major axis, and e is the eccentricity ($a = 1.95 \times 10^6$ km, $e = 0.617$ for PSR B1913+16). For our purpose, it is convenient to define the following 4 quadrupole moments, which are more closely connected

to the dynamics in the (x, y, z) frame:

$$\begin{aligned} Q_1(n) &= (\cos^2 \theta \cos^2 \phi - \sin^2 \phi) Q_{XX}(n) \\ &\quad - (\cos^2 \phi - \cos^2 \theta \sin^2 \phi) Q_{YY}(n), \end{aligned} \quad (6a)$$

$$Q_2(n) = \sin 2\phi (1 + \cos^2 \theta) Q_{XY}(n), \quad (6b)$$

$$Q_3(n) = 2 \cos \theta \cos 2\phi Q_{XY}(n), \quad (6c)$$

$$Q_4(n) = \cos \theta \sin 2\phi \left(Q_{XX}(n) - Q_{YY}(n) \right). \quad (6d)$$

For example, Eq. (3) can be rewritten as:

$$\begin{aligned} \frac{dE}{dt} &= \frac{\mu}{4} \sum_{n=1}^{\infty} (2\pi n f) \\ &\quad \left(-Q_1(n) \ddot{h}_{+} \sin(2\pi n f t) + Q_2(n) \ddot{h}_{+} \cos(2\pi n f t) \right. \\ &\quad \left. + Q_3(n) \ddot{h}_{\times} \cos(2\pi n f t) + Q_4(n) \ddot{h}_{\times} \sin(2\pi n f t) \right). \end{aligned} \quad (7)$$

Note that h_{\times} and h_{+} have identical statistical properties, and are uncorrelated. Strictly speaking, the orbital motion used on the right hand side of Eq. (7) to compute dE/dt should be the actual motion, accounting for both the orbital decay over time due to GW emission, and the orbital perturbation due to scattering with the external GWs. However, since both are very small effects, it is a very good approximation to use the unperturbed orbit.

Depending on the phase of the incoming strain, dE/dt can take either sign. Averaging over an ensemble of stochastic GWs would yield a vanishing change in the orbital energy of a detector binary; to find an observable signature of GWs, we must therefore compute the energy variance. Let ΔE be the energy change over some period of time T . It can be shown that its variance takes the form:

$$\langle \Delta E^2 \rangle = \sum_{i=1}^4 \sum_{n=1}^{\infty} \langle \Delta E_i^{(n)2} \rangle. \quad (8)$$

where i labels the energy change associated with the quadrupole Q_i . As an example, the $i = 3$ term is given by

$$\begin{aligned} \langle \Delta E_3^{(n)2} \rangle &= \left(\frac{\pi}{2} n f \mu \right)^2 \int_0^T dt \int_0^T dt' Q_3(n)^2 \langle \ddot{h}_{\times}(t) \ddot{h}_{\times}(t') \rangle \\ &\quad \cos(2\pi n f t) \cos(2\pi n f t') \\ &= T \mu^2 (\pi n f)^6 \frac{h_c(nf)^2}{2nf} Q_3(n)^2, \end{aligned} \quad (9)$$

$$\begin{aligned} \langle h_{\times}(t) h_{\times}(t') \rangle &= \langle h_{+}(t) h_{+}(t') \rangle \\ &= \frac{1}{2} \int_0^{\infty} \frac{df'}{f'} h_c^2(f') e^{i2\pi f'(t-t')}, \end{aligned} \quad (10)$$

with h_c^2 representing the (total) power spectrum per logarithmic frequency interval. We also assume $T \gg$

$1/(2\pi n f)$, and use:

$$\left| \int_0^T dt e^{i2\pi f' t} \cos(2\pi n f t) \right|^2 \approx \frac{T}{4} \delta(f' - n f). \quad (11)$$

A related delta function identity explains why different n modes do not mix in Eq. (8). The fact that different i 's do not mix is partly due to the fact that the two different polarizations are uncorrelated, and partly due to the fact that the analog of Eq. (11) for mixed sin and cos terms vanishes. Combining all terms, we have:

$$\langle \Delta E^2 \rangle = \frac{1}{2} \pi^6 T f^5 \mu^2 \sum_{n=1}^{\infty} n^5 h_c(n f)^2 \quad (12)$$

$$\left(Q_1(n)^2 + Q_2(n)^2 + Q_3(n)^2 + Q_4(n)^2 \right).$$

Using the virial relation: $E = -[G^2(m_1 + m_2)^2 f^2 \pi^2 / 2]^{1/3} \mu = -2\pi^2 f^2 a^2 \mu$, and the period $P = 1/f$, this can be rewritten as:²

$$\frac{\langle \Delta P^2 \rangle}{P^2} = \mathcal{A}^2 h_c(2f)^2 \frac{T}{P}, \quad (13)$$

with

$$\mathcal{A}^2 \equiv \frac{9\pi^2}{32} \sum_n n^5 \frac{h_c(n f)^2}{h_c(2f)^2} \times$$

$$a^{-4} \left(Q_1(n)^2 + Q_2(n)^2 + Q_3(n)^2 + Q_4(n)^2 \right). \quad (14)$$

The Q_i 's depend on the incidence direction of the GWs, so we average over (θ, ϕ) to find the net effect. However, it is worth noting that, even without averaging, $\langle \Delta E^2 \rangle$ or $\langle \Delta P^2 \rangle$ vary by at most a factor of 2 across the sky.

Eqs. (12) and (13) make clear that only harmonics of the orbital frequency f contribute to the rms energy/period change – the hallmark of a resonance effect. The singling out of these frequencies stems from delta functions like the one in Eq. (11), which has a width $\Delta f \sim 1/T$, where T is the duration of integration. We are interested in T from weeks to years (\gg the orbital period of 0.323 days for PSR B1913+16), corresponding to $\Delta f \sim 10^{-9} - 10^{-6}$ Hz. GWs within this width of the harmonics would contribute to the random walk of the binary elements.³

If the binary orbit is circular, only the $n = 2$ harmonic contributes, whereas for an eccentric orbit, all harmonics including $n = 1$ contribute in principle. In practice, the quadrupole moments $Q_i(n)$ decrease with n , and the expected rms strain h_c drops with frequency, which counteracts the strong n^5 dependence in Eqs. (12) and (13). Assuming $h_c \propto \text{freq.}^{-2/3}$ and the orbital parameters of PSR B1913+16, the dominant contributions come from $n = \{1, 4, 5, 3, 6, 7, 8, 2\}$, in order of importance, with the $n = 1$ mode contributing nearly as much as the other modes combined. Under the same assumptions, the dimensionless amplitude $\mathcal{A} \sim 10$. (Changing the spectrum to $h_c \propto \text{freq.}^{-1}$ would only change \mathcal{A} to ~ 10.25 .)

Eq. (13) thus tells us that

$$\frac{\Delta P_{\text{rms}}}{P} \sim 10 h_c(2f) \sqrt{\frac{T}{P}}, \quad (15)$$

which can be understood intuitively as follows. During each orbital period, the fractional change in period is roughly given by the strain h_c . The cumulative rms change scales up by the square root of the number of periods $\sqrt{T/P}$, as expected in a Brownian random walk. The extra factor of 10 depends on the details: the shape of the orbit and the spectrum of h_c – we choose to normalize at $2f$ (twice the orbital frequency) to facilitate comparison between different binaries, including circular ones.

III. DATA ANALYSIS

As a specific application of the generic method derived in the preceding section, we use PSR B1913+16 as the detector binary. The pulsar data carry a wealth of information about the system. For simplicity, we focus on the periastron time, recognizing that stronger constraints could potentially be obtained by analyzing the full time-of-arrival data, which we leave for future work. The periastron time data of PSR B1913+16 were published in [18]. They consist of 27 periastron time measurements, spanning from 1974 to 2006, each of which was obtained from monitoring the system over approximately 2 weeks (and ~ 2 hours per day over those 2 weeks). Let us label these times T_i , with i ranging from 1 up to N ($N = 27$ in our particular case). They can be modeled as follows:

$$T_i = \bar{T}_i + \Delta T_i + n_i, \quad (16)$$

where \bar{T}_i is a smooth component, ΔT_i is the excursion induced by GW scattering, and n_i represents noise. The smooth component takes the following form:

$$\bar{T}_i = \alpha + \beta p(i) + \gamma p(i)^2, \quad (17)$$

where $p(i)$ tracks the number of periods, known to high accuracy; α is the zero-point (we choose $p(1) = 0$); β is essentially the period and would be exactly the period if there was not a small change over time; γ quantifies the

² Note that when the system is being perturbed by the external GWs, the virial relation does not strictly hold on an instantaneous basis. However, when averaged over many orbits, we find the virial approximation of relating changes in energy to changes in period to be a very good one, with corrections suppressed by P/T ; here the period is defined in an average sense i.e. $2\pi = \int_T^{T+P(T)} \omega(t) dt$, as opposed to 2π divided by the instantaneous angular velocity ω .

³ The fact that the cumulative change in energy ΔE fluctuates, or random walks, can be understood as follows. As T varies, so does Δf , which controls which sources of gravitational waves contribute to resonant scattering with the detector binary. Since the sources have uncorrelated phases, ΔE undergoes random kicks as the relevant source population varies.

periastron shift due to the small change in the apparent period, induced by two smooth processes: (1) the famous decay of the orbit due to the *emission* of GWs, and (2) galactic acceleration of the system as a whole. Process (1) dominates over (2), though for our purpose there is no need to differentiate between them. Both are small compared to the zeroth-order effect i.e. $\gamma p(i)/\beta < 9 \times 10^{-8}$, and we will refer to β as the unperturbed period \bar{P} ; γ can be thought of as $\bar{P}\dot{\bar{P}}/2$ where $\dot{\bar{P}}$ is the rate of change of the period due to (1) and (2).⁴

The fluctuations due to noise n_i and due to GW scattering ΔT_i are uncorrelated, and their respective correlation matrices are

$$\langle n_i n_j \rangle = C_{ij} \quad , \quad \langle \Delta T_i \Delta T_j \rangle = h_c^2 (2f_{\text{HT}}) F_{ij} \quad , \quad (18)$$

where C_{ij} is the noise matrix, which we treat as diagonal using error bars from the data, and F_{ij} is defined as

$$F_{ij} \equiv \frac{1}{6} \mathcal{A}^2 \bar{P}^2 (\min[p(i), p(j)])^2 \\ (3 \max[p(i), p(j)] - \min[p(i), p(j)]) \quad . \quad (19)$$

To derive the expression for $\langle \Delta T_i \Delta T_j \rangle$, we use the fact that $\Delta T_i = \int_{T_1}^{T_i} dt \Delta P(t)/\bar{P}$, and compute $\langle \Delta P(t) \Delta P(t') \rangle$ using the same technique we used to compute $\langle \Delta P(t)^2 \rangle$ in Eq. (13).⁵ We also take advantage of the useful fact that $p(i) = \int_{T_1}^{T_i} dt/P(t)$, and the expressions above can be derived by noting that ΔP , ΔT_i and $\dot{\bar{P}}$ are small quantities. Henceforth, to avoid clutter, we suppress the i, j indices and use bold-faced symbols to represent matrices or vectors, wherever no confusion would arise.

It is worth pointing out that Eqs. (18) and (19) imply the rms fluctuation in periastron time, for $i = j$, is:

$$\Delta T_{\text{rms}} \sim 6 h_c (2f_{\text{HT}}) P \left(\frac{T}{\bar{P}} \right)^{3/2} \quad , \quad (20)$$

where we have abbreviated T_i as T , and \bar{P} as P . This result can be roughly thought of as coming from scaling Eq. (15) up by T . In other words, the rms fractional change in period *per period* is roughly the strain h_c ; after a number of periods given by T/P , the rms fractional change in period becomes $\sim h_c \times \sqrt{T/P}$; since the periastron time is cumulatively dependent on the period, the rms change in periastron time is $\sim h_c \times \sqrt{T/P} \times T$. It

is this rapid growth of ΔT_{rms} with time span T that we exploit to obtain constraints on h_c .

The minimum variance estimator for $\bar{\mathbf{T}}$ is [19]:

$$\bar{\mathbf{T}}_{\text{est.}} = \mathbf{L}(\mathbf{L}^T \mathbf{C}^{-1} \mathbf{L})^{-1} \mathbf{L}^T \mathbf{C}^{-1} \mathbf{T} \quad (21)$$

where \mathbf{L} is an $N \times 3$ matrix:

$$\mathbf{L} \equiv \begin{bmatrix} 1 & p(1) & p(1)^2 \\ 1 & p(2) & p(2)^2 \\ \vdots & \vdots & \vdots \\ 1 & p(N) & p(N)^2 \end{bmatrix} \quad . \quad (22)$$

The corresponding minimum variance estimator for the strain power spectrum h_c^2 at $2f$ is

$$h_{c, \text{est.}}^2 = \eta (\mathbf{T}^T \mathbf{W}^T \mathbf{C}^{-1} \mathbf{F} \mathbf{C}^{-1} \mathbf{W} \mathbf{T} - \Delta) \quad , \quad (23)$$

where the matrix \mathbf{W} is an $N \times N$ matrix defined by

$$\mathbf{W} \equiv \mathbf{1} - \mathbf{L}(\mathbf{L}^T \mathbf{C}^{-1} \mathbf{L})^{-1} \mathbf{L}^T \mathbf{C}^{-1} \quad , \quad (24)$$

and η and Δ are numbers defined by:

$$\eta \equiv 1/\text{Tr.} [\mathbf{C}^{-1} \mathbf{F} \mathbf{C}^{-1} \mathbf{W} \mathbf{F}^T \mathbf{W}^T] \quad , \quad (25)$$

$$\Delta \equiv \text{Tr.} [\mathbf{C}^{-1} \mathbf{F} \mathbf{C}^{-1} \mathbf{W} \mathbf{C} \mathbf{W}^T] \quad . \quad (26)$$

In deriving the above expressions, we have assumed the variance of the estimators are dominated by the noise n_i and not the signal ΔT_i . It can further be shown that the variance of estimator $h_{c, \text{est.}}^2$ is

$$\langle h_{c, \text{est.}}^4 \rangle - \langle h_{c, \text{est.}}^2 \rangle^2 = 2\eta \quad (27)$$

Because of the subtraction of the noise power spectrum (the Δ term), the estimated $h_{c, \text{est.}}^2$ can be negative, though its ensemble average cannot. Note also the estimate $h_{c, \text{est.}}^2$ implicitly assumes the shape of the power spectrum, through the quantity \mathcal{A} (see Eq. (14)) in the definition of F_{ij} . We will quote results assuming $h_c(f) \propto f^{-2/3}$. Assuming the power to go as f^{-1} would alter our results by a negligible amount compared to the uncertainties involved.

IV. RESULTS

From the periastron time data of PSR B1913+16 [18], we find the power per logarithmic frequency interval at $2f_{\text{HT}} = 7.2 \times 10^{-5}$ Hz to be $h_{c, \text{est.}}^2 = -6 \pm 7.4 \times 10^{-27}$. This is derived from fluctuations in the data after fitting and removing a smooth quadratic (see Eq. (17)). From this, we derive a 95% upper limit of $h_c < 7.9 \times 10^{-14}$ at 7.2×10^{-5} Hz.⁶

⁴ In most of the paper, we simply use P to denote the unperturbed period, when there is no danger of confusion.

⁵ We have implicitly assumed that the periastron time shift from external GWs is entirely due to their effect on the orbital period. In reality, there can be an (apparent) periastron time shift coming from center-of-mass linear momentum imparted by GWs, or from fluctuations in the orbital eccentricity. However, the former is suppressed by further powers of the orbital velocity, and the latter does not lead to a cumulative effect on the periastron time.

⁶ This upper limit corresponds to the value of h_c such that the probability of observing $h_{c, \text{est.}}^2$ at -6×10^{-27} or less is 5%.

Pulsars are known to have glitches, which are recognizable by abrupt changes in the spin period. The periastron timing data exhibit a large excursion around the glitch of May 2003, which we have removed from the above analysis. Had we included that data point, the results would not have changed significantly, as we would instead find $h_{c, \text{est.}}^2 = -3 \pm 7.4 \times 10^{-27}$.

V. DISCUSSION

Our GW constraint from the random walk of binary orbital elements raises several interesting issues. First, the constraint is a conservative one; namely, it is based upon a bound on fluctuations of the periastron data around a smooth curve. If there are additional sources of fluctuations other than scattering from the GW background, accounting for them would only strengthen our bound. However, a more thorough understanding of the possible sources of fluctuations would be necessary if one were to claim a detection of the GW background. Possibilities include glitches and tidal effects. Glitches are distinguished by accompanying fluctuations in the pulsar spin period, which are unlikely to have been caused by stochastic GWs. Tides cause secular changes of the binary dynamics rather than stochastic changes. To isolate the GW signal from other random or near-random processes, one can also take advantage of the well defined shape predicted for the two-point function of the periastron time fluctuations (see Eq. (18)).

The only other direct bound on GWs at a frequency $\sim 10^{-4}$ Hz comes from Doppler tracking of the *Cassini* spacecraft [20], which is roughly an order of magnitude more stringent than our constraint.⁷ Our bound is rather weak, especially when compared to the expected GW background from white-dwarf binaries, as shown in Fig. 1. The expected GW background is taken from [14], which is consistent with estimates such as [15, 16], though with a large uncertainty. Also shown is the expected sensitivity for the proposed eLISA/NGO/SGO detector [21].

Thus an important question is: how much do we expect the GW bound to improve from future observations of PSR B1913+16 and other binaries? To guide our think-

ing, we observe that the sensitivity of our method to the GW background scales as

$$\begin{aligned} h_c &\sim 5 \left(\frac{\delta T}{P} \right) N^{-1/2} \left(\frac{T_{\text{tot.}}}{P} \right)^{-3/2} \\ &\sim 5 \left(\frac{\delta T}{P} \right) n_P^{1/2} \left(\frac{T_{\text{tot.}}}{P} \right)^{-2}, \end{aligned} \quad (28)$$

where δT is the accuracy of each periastron time measurement, N is the number of such data points, P is the orbital period, $T_{\text{tot.}}$ is the total time span, and n_P is the number of periods between consecutive periastron time measurements, so that n_P^{-1} is the sampling rate.

The minimalist approach would be to simply lengthen $T_{\text{tot.}}$. Assuming the same rate of sampling as before (one periastron time data point per year), out to the year 2022, would push the sensitivity on h_c to 8.9×10^{-15} , comparable to the *Cassini* bound. This assumes $\delta T \sim 3 \times 10^{-8}$ day, which is about the level of accuracy towards the later years of the periastron data we analyzed [18].

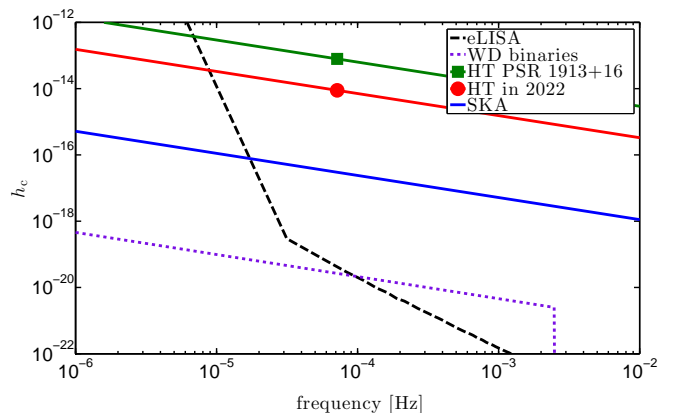


FIG. 1: Current constraint and future sensitivity on h_c , the square root of the strain power spectrum per logarithmic frequency. The uppermost line with the (red) square marker shows the current constraint from analyzing ~ 30 years of periastron time data from PSR 1913+16. The middle line with the (green) circle shows the expected sensitivity from the same system, if it continues to be observed ~ 2 hours per day for ~ 2 weeks each year until the year 2022. The bottom (blue) line shows the sensitivity from a hypothetical observational campaign employing the SKA to observe 100 binary systems (see text for details). In each case, the solid line going through the dot represents a $(\text{freq.})^{-2/3}$ spectrum which is assumed in deriving the bound. For comparison, we also show the expected strain sensitivity for eLISA/NGO/SGO [21] (dashed line), and the expected signal strength from white dwarf binaries [14] (dotted line) [14]. We caution that the white dwarf binary background has large uncertainties.

⁷ In our method, most of the constraining power of the data comes from the data points that are furthest apart i.e. $T \sim 32$ years, which corresponds to a fairly narrow frequency window of $\Delta f \sim 10^{-9}$ Hz. If one were to extrapolate this amplitude of h_c (7.9×10^{-14}) to a smooth spectrum over a broad bandwidth, one would obtain $\Omega_{GW} > 1$ which we know is ruled out by cosmological observations already. From this point of view, our bound is certainly weak. But it should be kept in mind that our bound on h_c applies strictly within a narrow frequency window, for which there is no useful cosmological bound. Note also that our bound is weak compared to the bound from big bang nucleosynthesis (BBN). However, once again, the BBN bound assumes a broad (scale invariant) spectrum of GWs, and it bounds GWs in the early universe and not from late time astrophysical sources.

A more ambitious approach would be to increase the sampling as well. Recall that the data we analyzed came from ~ 2 weeks of observations per year during which the pulsar was observed for only ~ 2 hours per day. This

is a fairly sparse sampling. What if we increase the sampling to one periastron time data point every 2 weeks (from 2012 to 2022)? The sensitivity on h_c then becomes 3.8×10^{-15} . Increasing the sampling is not as effective as increasing the total time span, but there is still some useful gain.

To go beyond this, let us consider the possibilities offered by the Square Kilometer Array (SKA). The SKA is expected to find hundreds of binaries with a pulsar member [22]. Let us assume 100 binaries, with an orbital period of around 0.1 day.⁸ The SKA also has a higher sensitivity than existing instruments. How much this translates into an improvement in the pulsar timing residual depends on how important the pulse jitter is, but an order of magnitude or so improvement is conceivable [23].⁹ Let us assume $\delta T \sim 10^{-9}$ day. (As an example, the periastron time data had improved in accuracy by almost two orders of magnitude from 1974 to 2006.) For the sampling, let us use $N = 100$ data points in the time span of 15 years. The projected sensitivity on h_c becomes $\sim 3 \times 10^{-17}$. This is also shown in Fig. 1.

There are a few open questions that remain to be explored. One is whether an even stronger GW bound can be obtained by analyzing the time-of-arrival data directly, as opposed to the periastron time data. There is a wealth of information in the time-of-arrival data, only a small fraction of which is captured by the periastron time. The question is whether, as far as the impact of external GWs on the test binary is concerned, most of the information is already contained in the periastron time data. For instance, we have not used any information about changes to the orbital eccentricity due to scattering with the external GWs, which can be deduced from the changes in energy and angular momentum (see Appendix). How much can our constraint improve if we use such information as well? Another interesting question is what current level of constraint we can obtain from other binary systems. Two in particular come to mind: the double pulsars PSR J0737-3039A/B, and the Earth-Moon system. A rough estimate for the double pulsar system, discovered in 2003, can be obtained by using $\delta T \sim 2 \times 10^{-7}$ day, $P \sim 0.1$ day, $T_{\text{tot.}} \sim 9$ years, $N \sim 30$ [24], giving a current sensitivity to h_c of $\sim 3 \times 10^{-13}$. This bound will improve more rapidly than the bound from the HT binary, since it has been observed for a shorter time. The Earth-Moon system is sensitive to the GW

background at a very different frequency: $\sim 8 \times 10^{-7}$ Hz. Laser-ranging to the moon can measure the Earth-Moon distance down to ~ 15 mm, which is a fractional accuracy of about 4×10^{-11} [25]. The main hurdle to obtaining accurate constraints on GWs is the need to model many geophysical effects of both the Earth and the Moon. A conservative bound can be obtained as long as one does not over-fit the lunar-ranging data.

Let us close by noting that our calculation applies strictly to a stochastic background. The case of super-massive black hole mergers needs to be separately considered, since their relative scarcity implies a GW signal more in the form of individual events, each of which is coherent. We hope to explore this in a future paper.

Acknowledgements

We thank Adam Brown, Fernando Camilo, Sergei Dubovsky, Eanna Flanagan, Eric Gotthelf, Zoltan Haiman, David Hogg, Mike Kesden, Vicky Kaspi, Michael Kramer, Szabi Marka, Wei-Tou Ni, Alberto Nicolis, Joel Weisberg and Matias Zaldarriaga for useful discussions. We are grateful to Jim Cordes for helpful discussions, and comments from Marc Kamionkowski that sharpened our explanation of several points. We especially thank Joe Taylor for providing the periastron time data and patiently answering many questions about them. This work was supported by the DOE, NASA and NSF under cooperative agreements DE-FG02-92-ER40699, NNX10AN14G, AST-0908365, and PHY11-25915. The work of I-Sheng Yang is supported in part by the Foundation for Fundamental Research on Matter (FOM), which is part of the Netherlands Organisation for Scientific Research (NWO).

Appendix A: Angular momentum

For completeness, we provide equations that describe the change of angular momentum due to scattering with the external GWs.

$$\begin{aligned} \frac{dL_x}{dt} &= \mu(-za_y) = \frac{1}{2}\mu(\ddot{h}_+yz - \ddot{h}_\times xz) , \\ \frac{dL_y}{dt} &= \mu(za_x) = \frac{1}{2}\mu(\ddot{h}_+xz + \ddot{h}_\times yz) , \\ \frac{dL_z}{dt} &= \mu(xa_y - ya_x) \\ &= \frac{1}{2}\mu(-2\ddot{h}_+xy + \ddot{h}_\times(x^2 - y^2)) , \end{aligned} \quad (\text{A1})$$

⁸ We envision binaries spanning a range of periods. Each thus probe the GW background at a different frequency. Assuming a spectrum for the background, we can bound a single number, i.e. the amplitude of the spectrum, using all the binaries. We assume the external GWs at the 100 binaries can be treated as uncorrelated. If there is some overlap in frequencies within the relevant resonant widths, there is the interesting possibility of cross-correlating excursions between binaries, which we leave for future work.

⁹ In cases where pulse jitter is important, improvement can only be achieved by longer integration.

Applying the same procedure as we did for the energy, the variance in the change in angular momentum is:

$$\langle(\Delta L_x)^2\rangle = \langle(\Delta L_y)^2\rangle = \frac{\pi^4}{8} T f^3 \mu^2 \sum_{n=1}^{\infty} n^3 h_c(nf)^2 \quad (\text{A2a})$$

$$\left(Q_5(n)^2 + Q_6(n)^2 + Q_7(n)^2 + Q_8(n)^2 \right),$$

$$\langle(\Delta L_z)^2\rangle = \frac{1}{2} \pi^4 T f^3 \mu^2 \sum_{n=1}^{\infty} n^3 h_c(nf)^2 \quad (\text{A2b})$$

$$\left(Q_1(n)^2 + Q_2(n)^2 + Q_3(n)^2 + Q_4(n)^2 \right),$$

where Q_5, Q_6, Q_7, Q_8 are defined by

$$Q_5(n) = \sin 2\theta \left(Q_{XX}(n) \cos^2 \phi + Q_{YY}(n) \sin^2 \phi \right),$$

$$Q_6(n) = \sin 2\phi \sin 2\theta Q_{XY}(n), \quad (\text{A3a})$$

$$Q_7(n) = 2 \sin \theta \cos 2\phi Q_{XY}(n), \quad (\text{A3b})$$

$$Q_8(n) = \sin \theta \sin 2\phi \left(Q_{XX}(n) - Q_{YY}(n) \right). \quad (\text{A3c})$$

The variance in the magnitude of \vec{L} is given by

$$\begin{aligned} \langle(\Delta|\vec{L}|)^2\rangle &= |\vec{L}|^{-2} \langle(\vec{L} \cdot \Delta\vec{L})^2\rangle \\ &= |\vec{L}|^{-2} \langle(L_x \Delta L_x + L_y \Delta L_y + L_z \Delta L_z)^2\rangle \\ &= |\vec{L}|^{-2} \left(L_x^2 \langle(\Delta L_x)^2\rangle + L_y^2 \langle(\Delta L_y)^2\rangle \right. \\ &\quad \left. + L_z^2 \langle(\Delta L_z)^2\rangle \right) \\ &= \sin^2 \theta \langle(\Delta L_x)^2\rangle + \cos^2 \theta \langle(\Delta L_z)^2\rangle. \quad (\text{A4}) \end{aligned}$$

-
- [1] V. N. Rudenko, *Sov. Astron.* **19**, 270 (1975).
[2] B. Mashhoon, *Astrophys. J.* **223**, 285 (1978).
[3] M. S. Turner, *Astrophys. J.* **233**, 685 (1979).
[4] B. Mashhoon, B. J. Carr, and B. L. Hu, *Astrophys. J.* **246**, 569 (1981).
[5] B. Bertotti, *Astrophys. Lett.* **14**, 51 (1973).
[6] C. W. Misner, K. S. Thorne, and J. A. Wheeler, *Gravitation* (W. H. Freeman, San Francisco, 1973).
[7] J. Weber, *Physical Review Letters* **22**, 1320 (1969).
[8] M. Kamionkowski, A. Kosowsky, and M. S. Turner, *Phys.Rev.* **D49**, 2837 (1994).
[9] R. Easther and E. A. Lim, *JCAP* **0604**, 010 (2006).
[10] J. F. Dufaux *et al.*, *Phys.Rev.* **D76**, 123517 (2007).
[11] J. Garcia-Bellido and D. G. Figueroa, *Phys.Rev.Lett.* **98**, 061302 (2007).
[12] E. Phinney, arXiv:astro-ph/0108028 (2001).
[13] A. J. Farmer and E. S. Phinney, *Mon.Not.Roy.Astron.Soc.* **346**, 1197 (2003).
[14] L. Barack and C. Cutler, *Phys. Rev. D* **70**, 122002 (2004).
[15] S. E. Timpano, L. J. Rubbo, and N. J. Cornish, *Phys. Rev. D* **73**, 122001 (2006).
[16] S. Nissanke, M. Vallisneri, G. Nelemans, and T. A. Prince, *Astrophys. J.* **758**, 131 (2012).
[17] P. C. Peters and J. Mathews, *Phys. Rev.* **131**, 435 (1963).
[18] J. M. Weisberg, D. J. Nice, and J. H. Taylor, *Astrophys. J.* **722**, 1030 (2010).
[19] G. B. Rybicki and W. H. Press, *Astrophys.J.* **398**, 169 (1992).
[20] J. W. Armstrong, L. Iess, P. Tortora, and B. Bertotti, *Astrophys. J.* **599**, 806 (2003).
[21] Final configurations of the ELISA(NGO) mission, <https://lisa-light.aei.mpg.de/bin/view/DetectorConfigurations/FinalConfiguration>.
[22] R. Smits *et al.*, *Astronomy and Astrophysics* **493**, 1161 (2009).
[23] K. Liu *et al.*, *Mon. Not. R. Astron. Soc.* **417**, 2916 (2011).
[24] M. Kramer *et al.*, *Science* **314**, 97 (2006).
[25] T. Murphy, Talk given at the Sackler Symposium (2012).